

Influence of the dielectric environment on the radiative lifetime of quantum-well excitons

D. Ammerlahn

Max-Planck-Institut für Festkörperforschung, D-70569 Stuttgart, Germany

B. Grote and S. W. Koch

Department of Physics and Materials Science Center, Philipps University, D-35032 Marburg, Germany

J. Kuhl and M. Hübner

Max-Planck-Institut für Festkörperforschung, D-70569 Stuttgart, Germany

R. Hey and K. Ploog

Paul-Drude-Institut für Festkörperelektronik, D-10117 Berlin, Germany

(Received 3 September 1999)

Due to the large mismatch in the refractive index of semiconductor material and air, time-integrated and spectrally resolved four-wave mixing experiments reveal strong influence of the cladding layer thickness, its refractive index, and the reflectivity of the sample-air interface on the radiative dephasing time of excitons in single quantum wells and multiple quantum well structures. A cladding layer thickness of $\lambda/2$ and $\lambda/4$ enhances and decreases, respectively, the radiative contribution to the exciton linewidth and causes radiative shifts to higher and lower energies, respectively. All our experiments are well described by solutions of the semiconductor Maxwell-Bloch equations.

I. INTRODUCTION

The coherent dynamic response of femtosecond excited excitons in semiconductor quantum wells (QW's) is determined by a variety of dephasing mechanisms. Scattering by other quasiparticles (phonons, excitons, free electrons, or holes) (Ref. 1) can be suppressed by choosing appropriate experimental conditions such as low temperatures and excitation densities. Dephasing due to minor sample quality, i.e., scattering by defects, interface roughness, or alloy fluctuations, should have been reduced by the modern growth techniques in the last decade. Surprisingly, the values reported for T_2 times of two-dimensional (2D) excitons in GaAs QW's seemed to be limited to less than 10–15 ps in spite of remarkable improvements of sample quality. Only recently, it has been shown that radiative recombination can provide a remarkable contribution to dephasing in high quality QW's in accordance with theoretical predictions for the radiative lifetime of 2D excitons published in several theoretical papers.^{2–4} In MQW Bragg structures, photon mediated coupling between excitons residing in neighboring QW's leads to strong enhancement of the radiative recombination rate so that radiative processes dominate the loss of phase coherence in such structures.^{5,6} It turned out that dephasing times depend strongly on the number of QW's N and the effective barrier thickness d^* .^{7,8} Even for a SQW, it has been predicted that the sample geometry plays an important role since it determines the interaction of the coherent exciton polarization with its own reemitted radiation field.⁹

In this paper, we show that the radiative lifetime and the transition energy of coherent 2D excitons are not inherent properties of the quantum well, but depend on its position inside the sample, especially on its distance from the sample surface, the reflectivity of the sample-air interface, and on

the refractive index of the cladding layer. This effect is caused by radiative recombination of the exciton and reflection of the emitted light at the sample-air interface. The phase difference between reflected light and the coherent exciton polarization in the QW and therefore the distance from the QW to the sample-air interface play an important role. If the cladding layer thickness is such that reflected light is in phase with the coherent exciton polarization, then the reflected light stimulates radiative emission, which leads to a shorter radiative lifetime and faster dephasing. If the reflected light has a phase difference of π to the exciton polarization, then additional polarization is created and the effective dephasing is slower. In reflectivity measurements on SQW's, it has been shown that depending on the effective cladding layer thickness d_1^* the exciton resonance can be both emissionlike for $d_1^* = m\lambda/2$ and absorptionlike for $d_1^* = (2m+1)\lambda/4$ (m integer).¹⁰ The same strong influence of the cladding layer thickness on reflectivity line shapes occurs for MQW Bragg structures.¹¹ In principle, the reflection from the backside of the sample has also to be taken into account. But in our case, the substrates are absorbing. Besides the cladding layer thickness, the reflectivity of the sample-air interface determines the magnitude of the changes of radiative dephasing and exciton energy. Therefore, under Brewster's angle, the polarization direction of the exciting laser pulses becomes critical for radiative dephasing due to the polarization dependence of the reflectivity. In the following, we exploit this polarization dependence for proving the high radiative contribution to excitonic dephasing and for confirming the theoretical value for radiative dephasing in the 2D limit as a lower limit for real QW excitons. Furthermore, we show that also for MQW's these considerations remain valid.

II. EXPERIMENTAL TECHNIQUES AND SAMPLES

In order to investigate the coherent dynamics of excitons in SQW's and MQW Bragg structures, we used degenerate four-wave mixing (DFWM) techniques. The optical pulses for resonant excitation of the excitonic transition were taken from a mode-locked Ti:sapphire laser, providing 100 fs pulses with an average power of 800 mW at a repetition rate of 76 MHz. With an external pulse shaper, we limited the bandwidth of the pulses to 2.4 meV in order to prevent simultaneous generation of the light-hole exciton or free carriers. The pulse length was thus extended to 800 fs. Low-energy pulses (5 pJ, focused to a spot size of 70 μm) with wavevectors \mathbf{k}_1 and \mathbf{k}_2 were used for DFWM in the two pulse self-diffraction geometry. Time-integrated (TI) measurements of the signal diffracted in direction $2\mathbf{k}_2 - \mathbf{k}_1$ were performed with a slow photodiode as a function of the delay τ_{12} between the two excitation pulses. For spectrally resolved (SR) experiments, we used a 0.75 m double monochromator with a resolution of 0.1 meV. The samples were held at a temperature of 8 K in a helium cryostat.

In order to prove the influence of sample-air interface reflection on excitonic dephasing, we turned the sample to Brewster's angle and compared DFWM signals generated with two laser beams that were polarized either parallel (p polarization) or perpendicular (s polarization) to the plane of incidence. Since there should be no reflection in the p polarization, we expect an influence of the surface reflection only for the s polarization. The different reflectivities of the two polarizations result in different exciton densities. For compensation, we doubled the laser intensity in the s polarization, which provides an approximately constant exciton density of about $10^8/\text{cm}^2$ in each case.

We used two samples grown by molecular-beam epitaxy. One consists of two different GaAs SQW's, a 15 nm QW and a 20 nm QW, separated by a 30-nm-thick $\text{Al}_{0.3}\text{Ga}_{0.7}\text{As}$ barrier. Since the exciton energies in these two QW's are separated by 8.3 meV, we can consider them to be independent from each other. Brewster's angle taken into account, the effective distance from the sample surface is $d_1^* = 0.33\lambda$ and $d_1^* = 0.53\lambda$ for the 15 nm QW and the 20 nm QW, respectively.

The second sample is a $N=10$ GaAs/ $\text{Al}_{0.3}\text{Ga}_{0.7}\text{As}$ Bragg structure with 20 nm well width. The 94.5-nm-thick (Al-Ga)As barriers yield a QW separation very close to $\lambda/2$ in the material at 8 K. It turned out⁶ that the QW spacing is slightly above $\lambda/2$. By increasing the angle α_{ext} between the bisector of the two laser beams and the growth direction of the sample, the effective well separation d^* is reduced as $d^* = d \cos(\alpha_{\text{int}}/\sqrt{\epsilon})$ with $\sin \alpha_{\text{ext}} = n_{\text{GaAs}} \sin \alpha_{\text{int}}$. The Bragg condition ($d^* = \lambda/2$) is fulfilled at $\alpha_{\text{ext}} = 49^\circ$.⁶ Since we mounted the samples under Brewster's angle ($\alpha_{\text{ext}} = 74^\circ$), the effective well separation of the Bragg sample is about $d^* = 0.49\lambda$. The effective thickness of the cladding layer amounts to $d_1^* = 0.24\lambda$.

III. THEORY

For modeling of the resonant interaction of an ultrashort light pulse propagating through a SQW or a MQW, the optical response of the interband polarization is calculated from

the semiconductor Bloch equations in Hartree Fock approximation while Maxwell's equations are solved to determine the self-consistent optical field. The externally applied field is renormalized by the retarded time derivatives of the induced interband polarizations within the different QW's.⁵ In MQW's, these polarization contributions to the local electric field lead to a radiative coupling between the different QW's. The semiconductor Maxwell-Bloch equations (SMBE) are iteratively solved up to third order in the electric field using the slowly varying envelope approximation and all contributions to the detected DFWM signal are picked out. In order to include the influence of sample disorder, a configuration average of the nonlinear response is performed.^{12,13}

The dephasing time T_2 of a QW exciton comprises radiative (γ_{rad}) and nonradiative (γ_0) contributions. In the exciton-pole approximation, the radiative dephasing rate in the 2D limit can be calculated by the dipole matrix element μ , the wavelength of the exciton transition in the medium λ , the refractive indices of the QW n_{QW} and the barrier material n_{bar} , and the overlap of the electron-hole wave function according to^{8,9}

$$\gamma_{\text{rad}}^{2\text{D}} = \frac{4\pi^2\mu^2}{\lambda} \frac{n_{\text{QW}}}{n_{\text{bar}}} |\varphi_{1S}^{2\text{D}}(0)|^2. \quad (3.1)$$

With the longitudinal-transverse splitting $\Delta_{\text{LT}} = 8\pi\mu^2|\varphi_{1S}^{3\text{D}}(0)|^2$ (Ref. 14), we can express $\gamma_{\text{rad}}^{2\text{D}}$ in experimentally accessible quantities:

$$\gamma_{\text{rad}}^{2\text{D}} = \frac{\pi\Delta_{\text{LT}}}{2\lambda} \frac{n_{\text{QW}}}{n_{\text{bar}}} \frac{|\varphi_{1S}^{2\text{D}}(0)|^2}{|\varphi_{1S}^{3\text{D}}(0)|^2}. \quad (3.2)$$

The overlap of the 2D and 3D exciton wave function is $8/\pi a_0^2$ and $1/\pi a_0^3$, respectively, with the Bohr radius of the exciton $a_0 = (n_{\text{QW}}^2 m_0/m_r) a_0^H$ (m_0 , electron mass; m_r , reduced exciton mass; $a_0^H = 0.529 \text{ \AA}$). Inserting the values corresponding to GaAs in Eq. (3.2) ($\hbar\Delta_{\text{LT}} = 0.08 \text{ meV}$, $\lambda = 818 \text{ nm}/n_{\text{bar}}$, $m_r = 0.06 m_0$, $n_{\text{QW}} = 3.63$, $n_{\text{bar}} = 3.44$), one obtains the radiative dephasing time $T_{\text{rad}}^{2\text{D}} = (\gamma_{\text{rad}}^{2\text{D}})^{-1} = 12.0 \text{ ps}$. The theoretical radiative linewidth in the 2D limit amounts to 0.11 meV. Since for $|\varphi_{1S}(0)|^2$ in real samples with finite QW width $|\varphi_{1S}^{3\text{D}}(0)|^2 < |\varphi_{1S}(0)|^2 < |\varphi_{1S}^{2\text{D}}(0)|^2$, $T_{\text{rad}}^{2\text{D}}$ represents a lower limit of real radiative dephasing times.

Equation (3.2) calculates γ_{rad} for a bare SQW and does not take into account any effect of surface reflection. As has been shown in Ref. 9, the effective radiative decay rate of a 2D exciton observed in an experiment is

$$\gamma_{\text{rad}}^* = \gamma_{\text{rad}} \left[1 + r \cos \left(4\pi \frac{d_1^*}{\lambda} \right) \right], \quad (3.3)$$

where γ_{rad} is the radiative dephasing rate for the bare QW and r is the reflection coefficient at the sample-air interface. According to Fresnel's equations and for incidence of the exciting laser beams on a semiconductor-vacuum interface at Brewster's angle, i.e., for $\alpha_{\text{ext}} + \alpha_{\text{int}} = 90^\circ$, r becomes 0 for p polarization and $-\cos 2\alpha_{\text{ext}}$ for s polarization yielding

$$\gamma_{\text{rad}}^{*p} = \gamma_{\text{rad}} \quad (3.4a)$$

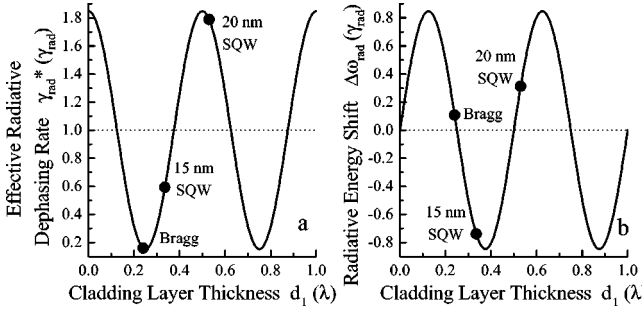


FIG. 1. Effective radiative dephasing rate (a) and radiative energy shift (b) in dependence on cladding layer thickness in terms of λ for laser beams with s polarization and incidence at Brewster's angle (GaAs, $\alpha_{\text{ext}} = 74^\circ$).

and

$$\gamma_{\text{rad}}^{*s} = \gamma_{\text{rad}} \left[1 - \cos 2\alpha_{\text{ext}} \cos \left(4\pi \frac{d_1^*}{\lambda} \right) \right]. \quad (3.4b)$$

γ_{rad}^{*s} is depicted versus d_1^* in Fig. 1(a) for GaAs (Brewster's angle $\alpha_{\text{ext}} = 74^\circ$). The shortest and longest lifetimes are expected for $d_1^* = m\lambda/2$ and $(2m+1)\lambda/4$ (m is an integer number), respectively, whereas for $d_1^* = (4m \pm 1)\lambda/8$ the influence of the surface should be negligible. Also the cladding layer thicknesses of our two SQW's and the Bragg sample with the corresponding effective radiative decay rates for s polarization are drawn in Fig. 1(a). The effect should go in opposite directions for the two SQW's.

In addition to the variation of radiative lifetimes, a slight radiative energy shift of the $1s$ exciton depending on the cladding layer thickness is predicted.⁹ At Brewster's angle, the shifts for p and s polarization are

$$\Delta\omega_{\text{rad}}^p = 0 \quad (3.5a)$$

and

$$\Delta\omega_{\text{rad}}^s = -\gamma_{\text{rad}} \cos 2\alpha_{\text{ext}} \sin \left(4\pi \frac{d_1^*}{\lambda} \right). \quad (3.5b)$$

For GaAs, the results obtained by using this formula are depicted in Fig. 1(b). As can be seen, shifts into opposite directions are predicted for the two SQW's.

It should be noticed that only the radiative dephasing rate γ_{rad} is affected by surface reflections. From TI-DFWM curves, one can deduce the homogeneous linewidth $2\hbar\gamma_{\text{hom}}$ that additionally contains the nonradiative contribution γ_0 ,

$$\gamma_{\text{hom}} = (T_2)^{-1} = (T_{\text{rad}}^*)^{-1} + (T_0)^{-1} = \gamma_{\text{rad}}^* + \gamma_0. \quad (3.6)$$

Therefore, only in high quality QW's with a small γ_0 compared to γ_{rad} , an effect of surface reflection is observable.

IV. RESULTS AND DISCUSSION

From Fig. 1(a), we extract the prediction that for all samples we should find differences between s and p polarization in the effective radiative dephasing rate and thus in the decay times of TI-DFWM signals. For the 20 nm QW, the effective radiative dephasing rate should be higher for s polarization, whereas for the 15 nm QW and the Bragg

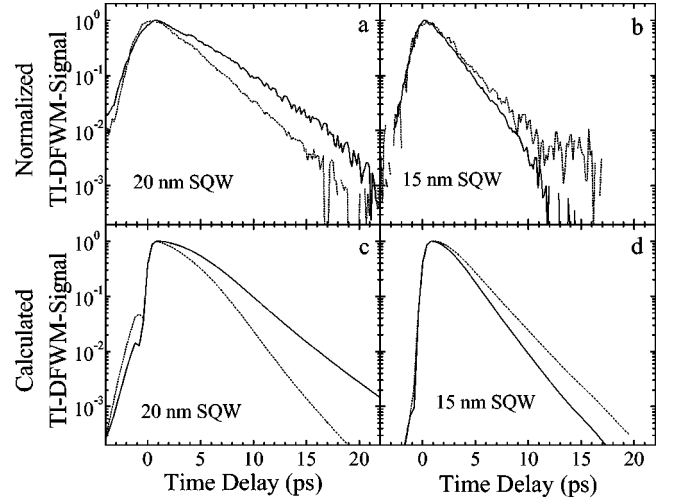


FIG. 2. TI-DFWM signals of SQW's at Brewster's angle for laser beams polarized parallel (solid curves) and perpendicular (dotted curves) to the plane of incidence: (a) 20 nm QW, (b) 15 nm QW, (c) and (d) corresponding calculations.

sample it should be lower. Figure 2(a) shows normalized TI-DFWM signals of the 20 nm SQW recorded at Brewster's angle with s (dotted line) and p polarization (solid line) of the exciting laser beams. The signal decay for the s polarization is clearly faster than for the p polarization. The TI-DFWM curves of the 15 nm QW, in contrast, show an opposite behavior [Fig. 2(b)]: for the s polarization the decay is slower than for the p polarization. The difference in the decay times is not as pronounced as for the 20 nm QW, and the decay of the coherent exciton polarization is faster than that of the 20 nm QW. This can be explained by minor quality of the 15 nm QW: the luminescence linewidth is 0.45 meV and thus a factor of 1.6 larger than the linewidth of the 20 nm QW.

In order to verify Eqs. (3.4), we analyze the TI-DFWM signal of the 20 nm QW. According to Eq. (3.4b), we expect for the effective cladding layer thickness $d_1^* = 0.53\lambda$ a larger radiative dephasing rate $\gamma_{\text{rad}}^{*s} = 1.8\gamma_{\text{rad}}$ for the s polarization. In general, the measured decay times τ_{dec} of TI-DFWM signals are equal to $T_2/2$ and $T_2/4$ for homogeneously and inhomogeneously broadened transitions, respectively.¹⁵ In the case of the 20 nm QW, the slope of both curves rises for increasing time delays. This occurs typically in the intermediate regime, where the inhomogeneous broadening σ_{inh} is comparable to the homogeneous linewidth $2\hbar\gamma_{\text{hom}}$: initially, the signal decays with $T_2/2$ and then the slope evolves continuously into $T_2/4$ for larger delays. In p polarization, we thus measure $T_2^p = 10$ ps, whereas dephasing for s polarization is remarkably faster ($T_2^s = 6.4$ ps). Considering the high quality of the 20 nm QW—its luminescence linewidth amounts to 0.29 meV—we can assume a rather small nonradiative contribution γ_0 to the total dephasing rate γ_{hom} . A lower limit for γ_0 of high quality QW's has been provided by the dephasing time of subradiant modes of a Bragg structure $T_2^{\text{sub}} = 38$ ps.¹³ From Eq. (3.6), we then calculate an effective radiative dephasing time $T_{\text{rad}}^{*s} = 7.7$ ps and $T_{\text{rad}}^{*p} = 13.6$ ps for the s and p polarizations, respectively, which agrees well with the expected factor of 1.8 between the dephasing rates of the two polarizations from Eqs. (3.4). For

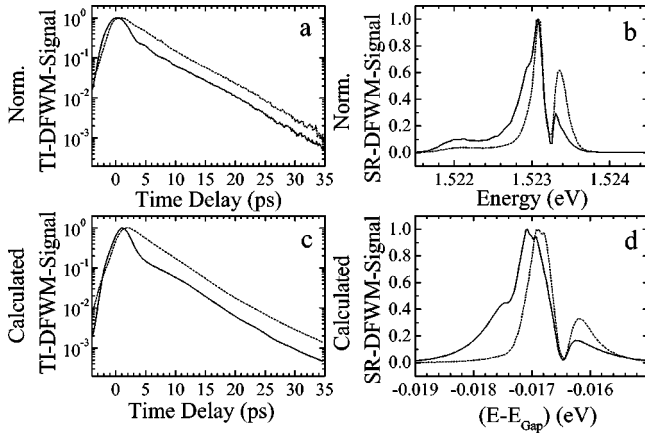


FIG. 3. TI-DFWM (a) and SR-DFWM (b) signals of a 10 QW Bragg structure at Brewster's angle for laser beams polarized parallel (solid curves) and perpendicular (dotted curves) to the plane of incidence. Calculated TI-DFWM (c) and SR-DFWM (d) curves.

the chosen values of T_2 and T_0 , however, we have to take into account relative errors of about 10% due to the difficult determination of T_2 in the intermediate regime between homogeneous and inhomogeneous broadening and to the assumption of T_0 . For the true radiative dephasing rate of a SQW, we then obtain $1/\gamma_{\text{rad}} = 14 \pm 2$ ps.

An analysis of the TI-DFWM curves of the 15 nm QW provides similar values, if one considers the minor quality compared to the 20 nm QW, which results in faster dephasing times. The larger inhomogeneous broadening gives rise to the approach of $\tau_{\text{dec}} = T_2/4$ and to a stronger nonradiative contribution ($T_0 \approx 13$ ps) to dephasing.

The calculated TI-DFWM curves in Figs. 2(c) and 2(d) show the same behavior as discussed above and agree quite well with the experimental curves. For the 20 nm QW, an inhomogeneous linewidth $\sigma_{\text{inh}} = 0.29$ meV and a nonradiative dephasing rate of $\gamma_0 = 0.017$ meV/ \hbar ($T_0 = 38$ ps) have been chosen. The parameters for the 15 nm QW were $\sigma_{\text{inh}} = 0.45$ meV and $\gamma_0 = 0.058$ meV/ \hbar ($T_0 = 11.3$ ps).

For a perfect Bragg sample with N QW's, the radiative dephasing rate $\gamma_{\text{rad}}^{\text{Bragg}}$ amounts to N times the radiative dephasing rate of a SQW γ_{rad} . Therefore, one expects stronger influence of the surface reflection and larger differences between the two polarizations for the Bragg sample than for the SQW's. As we have shown in previous papers,^{5-7,12,13,16} the TI-DFWM signal of a Bragg structure containing a certain amount of disorder or being slightly detuned from the Bragg condition $d^* = \lambda/2$ is first dominated by a fast superradiant mode and at later times by slower subradiant modes. Superposition results in approximately biexponentially decaying TI-DFWM signals. The fast decay time of the superradiant mode rests upon exciton recombination stimulated by photons sent out from neighboring QW's, whereas the subradiant mode is mainly determined by nonradiative dephasing processes. Since the influence of surface reflection on the radiative dephasing rate is a mere radiative effect, we only expect a significant change in the superradiant mode.

TI-DFWM curves of our Bragg sample in Figs. 3(a) and 3(c) show a qualitatively different behavior during the first 4 ps depending on the polarization direction of the excitation pulses. While a superradiant decay can be observed for the p

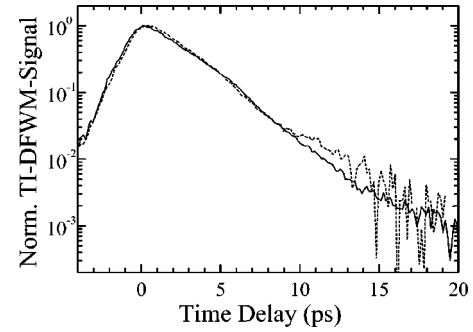


FIG. 4. TI-DFWM signals of the GaAs bulk exciton at Brewster's angle for laser beams polarized parallel (solid curves) and perpendicular (dotted curves) to the plane of incidence.

polarization, the creation of a superradiant mode is suppressed for the s polarization due to the strong reflection at the sample-air interface leading to a relative phase of nearly π ($d_1^* \approx \lambda/4$) of the optical field coupled back into the Bragg structure. The long-time behavior of the TI-DFWM traces show almost the same behavior for s and p polarization since it is dominated by subradiant modes with small radiative broadening compared to the superradiant mode and even to the SQW.^{12,13}

This behavior can also be seen in the SR-DFWM curves of the Bragg structure [Figs. 3(b) and 3(d)]. The broad background due to the superradiant mode in the p polarization visible in the low-energy part of the spectrum vanishes for the s polarization. As we have shown previously,¹⁷ the subradiant modes manifest themselves in SR-DFWM as a dip in backward direction and a spike in forward direction. Performing our experiments in backward diffraction geometry, we observe in Fig. 3(b) that the dip in the spectra remains at the same energetic position, whereas the center of the spectrum is shifted towards higher energies for the s polarization. The energy shift was predicted by Eqs. (3.5), and the direction of the shift to higher energies was depicted in Fig. 1.

The analysis of the superradiant mode in the p polarization, which is homogeneously broadened,¹³ yields with $T_0 = 38$ ps an effective radiative dephasing time of approximately $T_{\text{rad}}^{\text{exp}} = T_{\text{rad}}^{*p} = 3.3$ ps. With a radiative dephasing time of 14 ps derived above for a SQW, one would expect for a perfect Bragg structure with 10 QW's $T_{\text{rad}}^{\text{theo}} \approx 1.4$ ps. The discrepancy between $T_{\text{rad}}^{\text{theo}}$ and $T_{\text{rad}}^{\text{exp}}$ can be explained by sample disorder ($\sigma_{\text{inh}} = 0.5$ meV) in real samples and by the fact that our sample is about 1.6% detuned from the Bragg condition $d^* = \lambda/2$. Both effects tend to destroy the superradiant coupling of the excitons in different QW's and slow down the superradiant decay of the DFWM signal.

The interaction of the coherent exciton polarization with its own reemitted radiation field is a mere 2D phenomenon. As can be seen in Fig. 4, TI-DFWM measurements on the GaAs bulk exciton show no differences in the decay times for p and s polarization ($\tau_{\text{dec}} \approx 2.5$ ps). Since 3D excitons have no direct radiative decay channel due to momentum conservation, their radiative lifetime is much larger than for 2D excitons, and their dephasing is dominated by other mechanisms. Thus, the coherent bulk exciton polarization remains almost unaffected by radiation reflected from the sample-air interface. Furthermore, the excitonic excitation in bulk material is not localized. Different distances to

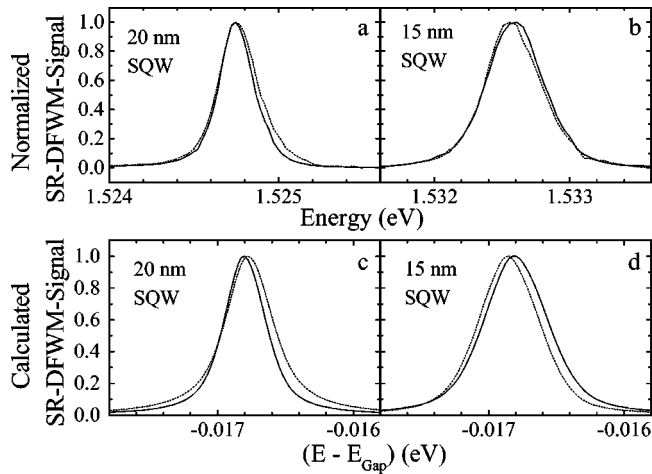


FIG. 5. SR-DFWM signals of SQW's at Brewster's angle for laser beams polarized parallel (solid curves) and perpendicular (dotted curves) to the plane of incidence: (a) 20 nm QW, (b) 15 nm QW, (c) and (d) corresponding calculations.

the surface lead then to all possible phase differences between exciton polarization and reflected radiation so that in average the radiative dephasing rate remains unchanged. This affirms that the observed different decay times of coherent QW excitons for s and p polarization are due to a pure radiative effect.

As to the SR-DFWM measurements of the 20 nm and 15 nm QW's in Figs. 5(a) and 5(b), respectively, we find that the energy shifts are very small. According to Eq. (3.5b) and with the experimentally found $T_{\text{rad}} \approx 14$ ps ($\hbar \gamma_{\text{rad}}$

≈ 0.05 meV), one would expect an energy shift for s polarization of about 0.02 meV to higher and 0.04 meV to lower energies for the 20 nm and 15 nm QW, respectively. Since this is very close to the resolution of our spectrometer, we abandon an exact analysis of the shifts. However, by comparing the measured spectra with the calculated spectra in Figs. 5(c) and 5(d), one can see that the exciton energies are shifted in the predicted directions.

V. CONCLUSIONS

In conclusion, we have demonstrated a remarkable influence of the cladding layer thickness, its refractive index and the reflectivity of the sample-air interface on radiative dephasing of 2D excitons. TI- and SR-DFWM experiments on high quality QW's revealed different radiative dephasing rates and radiative energy shifts for s - and p -polarized exciting laser beams at Brewster's angle. Analysis of our experimental data provides radiative dephasing times of about 14 ± 2 ps for excitons in SQW's. A theoretical lower limit of real radiative dephasing times in the 2D limit is given by 12.0 ps for GaAs parameters. For MQW Bragg structures, the changes in the radiative dephasing rate are enhanced according to the number of QW's. All our experiments are well described by solutions of the SMBE.

ACKNOWLEDGMENTS

Different parts of this project have been funded by the Deutsche Forschungsgemeinschaft, the Sonderforschungsbereich 383, and the Leibniz prize.

- ¹L. Schultheis, J. Kuhl, A. Honold, and C.W. Tu, Phys. Rev. Lett. **57**, 1635 (1986).
- ²E.L. Ivchenko, A.I. Nesvizhskii, and S. Jorda, Phys. Solid State **36**, 1156 (1994).
- ³E. Hanamura, Phys. Rev. B **38**, 1228 (1988).
- ⁴L.C. Andreani, F. Tassone, and F. Bassani, Solid State Commun. **77**, 641 (1991).
- ⁵T. Stroucken, A. Knorr, and S.W. Koch, Phys. Rev. B **53**, 2026 (1996).
- ⁶M. Hübner, J. Kuhl, T. Stroucken, A. Knorr, S.W. Koch, R. Hey, and K. Ploog, Phys. Rev. Lett. **76**, 4199 (1996).
- ⁷J. Kuhl, M. Hübner, D. Ammerlahn, T. Stroucken, B. Grote, S. Haas, S.W. Koch, G. Khitrova, H.M. Gibbs, R. Hey, and K. Ploog, in *Festkörperprobleme/Advances in Solid State Physics*, edited by B. Kramer (Vieweg, Braunschweig, 1998), Vol. 38, p. 281.
- ⁸T. Stroucken, S. Haas, B. Grote, S.W. Koch, M. Hübner, D. Ammerlahn, and J. Kuhl, in *Festkörperprobleme/Advances in Solid State Physics* (Ref. 7), p. 265.
- ⁹S. Haas, T. Stroucken, M. Hübner, J. Kuhl, B. Grote, A. Knorr, F. Jahnke, S.W. Koch, R. Hey, and K. Ploog, Phys. Rev. B **57**, 14 860 (1998).
- ¹⁰X.L. Zheng, D. Heiman, B. Lax, and F.A. Chambers, Appl. Phys. Lett. **52**, 287 (1988).
- ¹¹Y. Merle d'Aubigné, A. Wasiela, H. Mariette, and T. Dietl, Phys. Rev. B **54**, 14 003 (1996).
- ¹²B. Grote, T. Stroucken, S. Haas, P. Thomas, and S.W. Koch, Phys. Status Solidi B **205**, 209 (1998).
- ¹³M. Hübner, J. Kuhl, B. Grote, T. Stroucken, S.W. Koch, R. Hey, and K. Ploog, Solid State Commun. **108**, 787 (1998).
- ¹⁴H. Haug and S.W. Koch, *Quantum Theory of the Optical and Electronic Properties of Semiconductors* (World Scientific, Singapore, 1993).
- ¹⁵T. Yajima and Y. Taira, J. Phys. Soc. Jpn. **47**, 1620 (1979).
- ¹⁶M. Hübner, J. Kuhl, B. Grote, T. Stroucken, S. Haas, A. Knorr, S.W. Koch, G. Khitrova, and H. Gibbs, Phys. Status Solidi B **206**, 333 (1998).
- ¹⁷D. Ammerlahn, J. Kuhl, M. Hübner, B. Grote, T. Stroucken, S.W. Koch, G. Khitrova, and H. Gibbs, in *Ultrafast Phenomena XI*, edited by T. Elsaesser, J.G. Fujimoto, D.A. Wiersma, and W. Zinth (Springer, Berlin, 1998).